

[Re]CUDA:Curriculum of Data Augmentation for Long-Tailed Recognition

Anonymous authors

Paper under double-blind review

Abstract

In this reproducibility study, we present our results and experience during replicating the paper, titled CUDA: Curriculum of Data Augmentation for Long-Tailed Recognition (Ahn et al., 2023). Traditional datasets used in image recognition, such as ImageNet, are often synthetically balanced, meaning each class has an equal number of samples. In practical scenarios, datasets frequently exhibit significant class imbalances, with certain classes having a disproportionately larger number of samples compared to others. This discrepancy poses a challenge for traditional image recognition models, as they tend to favor classes with larger sample sizes, leading to poor performance on minority classes. CUDA proposes a class-wise data augmentation technique which can be used over any existing model to improve the accuracy for LTR: Long Tailed Recognition. We successfully replicated a substantial portion of the results pertaining to the long-tailed CIFAR-100-LT dataset and extended our analysis to provide deeper insights into how CUDA efficiently tackles class imbalance.

1 Introduction

Long-tailed recognition presents one of the most formidable challenges in visual recognition. This problem revolves around training highly effective models from datasets characterized by a large number of images distributed along a long-tailed class distribution. In datasets characterized by class imbalance, a notable skew exists in the distribution of samples across different classes, resulting in certain classes being vastly over-represented (Head classes) while others are significantly under-represented (Tail classes). To elucidate this phenomenon, consider a practical example in the domain of disease screening tests: the head classes primarily comprise instances of non-patients, whereas the tail classes represent the minority of patients. In such scenarios, the performance of deep learning models tends to be disproportionately influenced by the Head classes, while the learning of Tail classes is often inadequately developed.

Solutions to Long Tailed recognition primary involves three methods: (1) Resampling (Buda et al., 2018): up-sampling minority classes and Down-sampling majority classes. (2) Reweighting (Cao et al., 2019): rebalancing the loss to give more weights to minority classes. (3) Transfer learning (Kim et al., 2020): enriching the information of minority classes by transferring information gathered from majority classes to the minority classes. While numerous strategies have been suggested to leverage data augmentation techniques for generating diverse representations of minority samples, scant attention has been given to assessing the impact of varying augmentation degrees across different classes on addressing class imbalance issues.

The original authors propose that applying an algorithm to determine class-wise augmentation strength can potentially address the imbalance problem in long-tailed visual recognition tasks. This data augmentation technique called CUDA is designed to complement existing Long-Tailed Recognition (LTR) models. The other key finding, as highlighted in the original paper, is that after training when we examine the class-wise strength of augmentation the majority classes have a stronger degree of augmentation and the minority classes have a weaker degree of augmentation. This finding is counter-intuitive, as one would typically anticipate that the minority class, with fewer samples, would undergo strong augmentation, while the majority class, with more samples, would undergo weaker augmentation. The original authors utilized two metrics, weight L1-norm and feature alignment gain, to demonstrate the effectiveness of CUDA in mitigating the imbalance

problem. However, the original authors did not elaborate on how these two metrics are linked to the feature representation of imbalanced datasets or elucidate how CUDA influences the feature representation space.

The motivation behind this reproducibility study is threefold: (1) To validate the assertion made by the original authors that employing class-wise augmentation strength can enhance performance of existing LTR models. (2) To confirm the counter-intuitive observation from the original paper that employing stronger augmentation on majority classes and milder augmentation on minority classes yields superior model performance compared to the opposite strategy. (3) To delve deeper into how CUDA effectively addresses the imbalance problem by leveraging insights from prior research on feature representations in long-tailed datasets, a dimension not explored in the original paper.

2 Scope of Reproducibility

To address our threefold motivation behind this paper and to reproduce the results of the original paper, we perform the following experiments over the CIFAR-100-LT dataset:

1. For our first motivation, we examine the performance of CUDA across LTR models like CE (Cross Entropy), CE-DRW (Cross entropy Dynamic reweighting), LDAM-DRW (label-distribution-aware margin loss), BS (balanced softmax) and RIDE (Figure 3).
2. For our second motivation, we investigate the LOL (Learning Objective Level) score, representing the augmentation strength of each class after training with CUDA (Figure 4).
3. We examine how accuracy changes with the three hyper-parameters augmentation probability, number of test samples, and acceptance rate to reproduce the result that both excessive and insufficient augmentation adversely affect performance (Figure 7).
4. We examine the metrics variance of weight L1-norm and feature alignment gain to reproduce the result that CUDA leads to a decrease in weight L1-norm and a positive feature alignment gain (Figure 5 and Figure 6).
5. We evaluate the contribution of curriculum learning and class-wise score on the performance of CUDA to reproduce the result that both curriculum learning and class-wise score are important to the performance of CUDA (Figure 8).
6. We compare the performance of CUDA with other augmentation methods to validate the result that CUDA outperforms all existing augmentation techniques (Figure 8).
7. We conduct the performance analysis across three different imbalance ratios (100, 50, 10) to examine how CUDA performance varies with dataset imbalance ratios (Figure 10).
8. For our third motivation, we compare the feature representation space of the vanilla and CUDA versions, examining metrics such as inter-class distance and intra-class distance (Figure 9).

3 Methodology

3.1 Model descriptions

We use Resnet-32 as our backbone model for all 5 models CE, CE-DRW, BS, LDAM-DRW, and RIDE. However RIDE uses modified version of Resnet-32 implemented according to the original paper. We use the data augmentation technique CUDA over these existing 5 models. The core philosophy of CUDA is to “generate an augmented sample that becomes the most difficult sample without losing its original information”. CUDA uses two main parts to achieve this: (1) Strength-based augmentation (2) Using Level-of-Learning (LOL) score. In following sections 3.1.1 and 3.1.2 we explain the methodology of CUDA as outlined in the original paper.

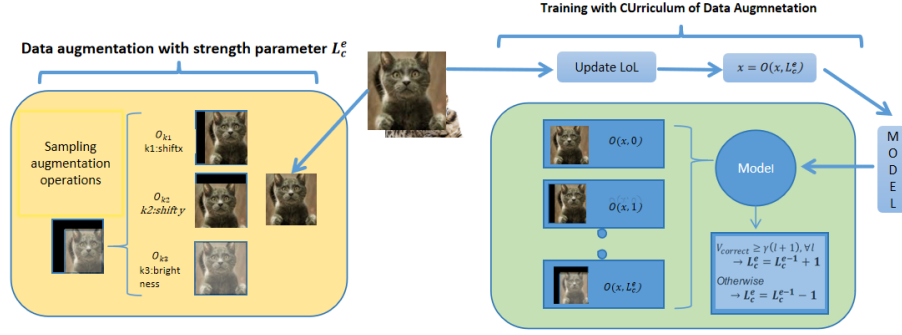


Figure 1: Schematic of CUDA. The left part depicts the strength based augmentation and the right part depicts how the Level-of-Learning (LOL) score is updated in a given epoch

3.1.1 Strength-based augmentation

We need to define a metric to quantify the degree of augmentation we are applying on an image. Let us assume that there exists K predefined augmentation operations indexed as $k \in \{1, \dots, K\}$, for example gaussian blur, rotation, horizontal flip etc. Each augmentation operation $O_k^{m_k(s)}$ has its own predefined augmentation magnitude function $m_k(s)$ with the strength parameter $s \in \{0, \dots, S\}$. Given an augmentation strength parameter s and an input image x , we model a sequence of augmentation operations $O(x; s)$ as follows:

$$O(x; s) = O_{k_s}^{m_{k_s}(s)} \circ O_{k_{s-1}}^{m_{k_{s-1}}(s)} \circ \dots \circ O_{k_1}^{m_{k_1}(s)}(x), \quad k_i \sim \text{Cat}(K, \mathcal{U}(K)) \quad \forall i = \{1, \dots, s\}$$

The sequential augmentation operation $O(x; s)$ involves sampling s operations from a categorical distribution, where each operation is chosen from a uniform distribution among K possible operations. In essence, out of the K possible operations, only s operations are selected, each with a magnitude $m(3)$. For example, let's consider $s = 3$. Suppose the selected augmentation operations k_1, k_2, k_3 correspond to brightness adjustment, x-shift, and y-shift, respectively. In this case, $O(x; 3)$ outputs an image where the brightness is increased by $m_{\text{bright}}(3)$, shifted by $m_{x\text{-shift}}(3)$ on the x-axis and shifted by $m_{y\text{-shift}}(3)$ on the y-axis. As s increases, both the number of augmentation operations applied to each image and the magnitude of each of these operations increase consequently, the complexity of the augmentation process increases. Appendix-A on augmentation preset describes how $m_k(s)$ the magnitude function of each data augmentation operation is defined.

3.1.2 Updating Level of Learning Score

To control the strength of augmentation properly, we need to check whether the model can correctly predict augmented versions without losing the original information. To enable this, we define the LOL for each class c at epoch e , i.e., L_c^e which is adaptively updated as the training continues as follows:

- Initialization: At the start of training, set L_c^e to zero for all classes. For clarity, let's consider that two epochs have already passed, and we begin at the third epoch. Let's assume L_1^2 the LOL score for a specific class 1 after the second iteration is 2.
- Update Mechanism: The LOL value for each class is updated using the function V_{lol} , which takes inputs such as the images D_c belonging to class c , the previous LOL value L_c^{e-1} , the model f_θ used for prediction, and hyper parameters γ and T .

$$L_c^e = V_{LoL}(D_c, L_c^{e-1}, f_\theta, \gamma, T)$$

- Sampling : Within V_{lol} we iterate over all values of l less than $L_1^2 = 2$. For each l (0, 1, 2 in this case), randomly sample $T(l+1)$ samples from D_c to form D'_c , ensuring $|D'_c| = T(l+1)$. Instead of utilizing all samples in set D_c for prediction, we opt for a subset of images denoted as D'_c . The

Algorithm 1: CUrriculum of Data Augmentation	Algorithm 2: V_{LoL} : Update LoL score
Input: LTR algorithm $\mathcal{A}_{\text{LTR}}(f, \mathcal{D})$, training dataset $\mathcal{D} = \{(x_i, y_i)\}_{i=1}^N$, train epochs E , aug. probability p_{aug} , threshold γ , number of sample coefficient T . Output: trained model f_θ Initialize: $L_c^0 = 0 \forall c \in \{1, \dots, C\}$ for $e \leq E$ do Update $L_c^e = V_{\text{LoL}}(\mathcal{D}_c, L_c^{e-1}, f_\theta, \gamma, T) \quad \forall c \quad // \text{ Alg. 2}$ Generate $\mathcal{D}_{\text{CUDA}} = \{(\bar{x}_i, y_i) (x_i, y_i) \in \mathcal{D}\}$ where $\bar{x}_i = \begin{cases} \mathcal{O}(x_i, L_{y_i}^e) & \text{with prob. } p_{\text{aug}} \\ x_i & \text{otherwise.} \end{cases}$ Run LTR algorithm using $\mathcal{D}_{\text{CUDA}}$, i.e., $\mathcal{A}_{\text{LTR}}(f_\theta, \mathcal{D}_{\text{CUDA}})$. end	Input: $\mathcal{D}_c, L, f_\theta, \gamma, T$ Output: updated L Initialize: check = 1 for $l \leq L$ do /* $V_{\text{correct}}(\mathcal{D}_c, l, f_\theta, T)$ */ Sample $\mathcal{D}'_c \subset \mathcal{D}_c$ s.t. $ \mathcal{D}'_c = T(l+1)$ Compute $v = \sum_{x \in \mathcal{D}'_c} \mathbb{1}_{\{f(\mathcal{O}(x; l))=c\}}$ if $v \leq \gamma T(l+1)$ then check $\leftarrow 0$; break end end if check = 1 then $L \leftarrow L + 1$ else $L \leftarrow L - 1$

Figure 2: Algorithm of CUDA (Ahn et al., 2023)

size of this subset is determined by the first hyper parameter, denoted as T , which represents the number of test samples.

- Calculation of V_{correct} : This involves summing the indicator function $\mathbb{1}_{f_\theta(\mathcal{O}(x; l))=c}$ for all samples in \mathcal{D}'_c , where $\mathcal{O}(x; l)$ represents the application of augmentation strength l to sample x . If the model correctly predicts class c ($c=1$ in this case), the function evaluates to 1. In essence, V_{correct} quantifies the number of correct predictions among the $T(l+1)$ samples in \mathcal{D}'_c .

$$V_{\text{Correct}}(\mathcal{D}_c, l, f_\theta, T) = \sum_{x \in \mathcal{D}'_c} \mathbb{1}_{\{f_\theta(\mathcal{O}(x; l))=c\}} \quad \text{where } \mathcal{D}'_c \subset \mathcal{D}_c$$

- Adjustment: If the number of correct predictions exceeds the threshold $\gamma \cdot T(l+1)$, where l takes values from 0 to 2, it signifies that the ratio of correct predictions to total samples surpasses the second hyper parameter γ , representing the acceptance rate. In this scenario, the value of the LOL score for the next epoch, denoted as L_1^3 , is incremented by 1 compared to the current value of L_1^2 ($L_1^3 = L_1^2 + 1 = 3$). If the condition is not met, the value of LOL score is decremented by 1 ($L_1^3 = L_1^2 - 1 = 1$)

$$V_{\text{LoL}}(\mathcal{D}_c, L_c^{e-1}, f_\theta, \gamma, T) = \begin{cases} L_c^{e-1} + 1 & \text{if } V_{\text{Correct}}(\mathcal{D}_c, l, f_\theta, T) \geq \gamma T(l+1) \quad \forall l \in \{0, \dots, L_c^{e-1}\} \\ L_c^{e-1} - 1 & \text{otherwise} \end{cases}$$

- Augmentation Sequence: By applying V_{lol} for all classes we could then define a sequence of augmentation operations $\mathcal{O}(x_i, L_{y_i}^e)$ with their strengths defined by the respective $L_{y_i}^e$ where each y_i is a class.
- Augmentation Probability: Instead of completely replacing the training dataset \mathcal{D} with augmented images, we apply a sequence of augmentation operations with a probability specified by a third hyper parameter, ρ , representing the augmentation probability. This results in the creation of a new dataset $\mathcal{D}_{\text{CUDA}}$.
- LTR algorithm: Execute any Learning to Rank (LTR) algorithm utilizing the dataset $\mathcal{D}_{\text{CUDA}}$, comprising both augmented and original images.

3.2 Dataset and Hyper Parameters

The reproduction study is done on the dataset CIFAR-100-LT as mentioned in the previous works(Cao et al., 2019).The CIFAR-100 dataset (Canadian Institute for Advanced Research, 100 classes) is a subset

of the Tiny Images dataset and consists of 60000 32x32 color images. Three different datasets are derived from CIFAR-100 dataset with imbalance ratio 100, 50 and 10, where an imbalance ratio is defined as $|D_1|/|D_{100}| = N_{\max}/N_{\min}$. $|D_k|$ between $|D_1| = N_{\max}$ and $|D_{100}| = N_{\min}$ follows an linear decay. The hyper-parameters augmentation probability, number of test samples and acceptance rate are used as mentioned in the original paper. The values used are 0.6 for augmentation probability, 10 for number of test samples and 0.5 for Acceptance rate. The hyper parameter sensitivity analysis done on Section 4.1.5 for the three hyper parameters further substantiated the values used.

3.3 Experimental setup and code

We have conducted all experiments for the dataset CIFAR-100-LT by using the official repository, which is implemented in PyTorch. The code from the repository was reorganized into a Jupyter notebook to enhance portability and offer better control over the environment. The dependencies were not explicitly provided, and the versions of different libraries were determined through trial and error. Deprecated elements within the code were replaced with suitable, up-to-date alternatives. For training the model, parameters were set based on the specifications outlined in the paper. Any parameters not explicitly mentioned in the paper were assumed to use default values. The code for conducting component analysis on curriculum learning, class-wise score measurement and measuring the standard deviation in weight L1 norm were re-implemented based on the specifications provided in the paper. The code and the readings are available here.

3.4 Computational requirements

We trained the model in kaggle with 1 NVIDIA Tesla P100 as the GPU accelerator. The average training time of the model was approximately 40 minutes with a batch size of 128 for 200 epochs and the overall budget of the reproduction study was 250 GPU hours.

4 Results

4.1 Results reproducing original paper

Section 4.1.1 delves into the findings related to the first motivation of validating the assertion made by the original authors that employing class-wise augmentation strength can enhance performance of existing LTR models. Section 4.1.2 delves into the findings related to the second motivation of confirming the counter-intuitive observation from the original paper that employing stronger augmentation on majority classes and milder augmentation on minority classes yields superior model performance compared to the opposite strategy. Section 4.1.3 and section 4.1.4 provides additional insights on the original study on weight L1 norm and feature alignment gain that also justifies our third motivation of investigating feature representations in long-tailed datasets. The subsequent sections in 4.1 encompass the results obtained from our reproduction of various analytical studies conducted in the original paper, aiming to further validate and understand the efficacy and implications of employing CUDA.

4.1.1 Comparison of validation accuracy

We measure the validation accuracy of CUDA when used with CE (Cross Entropy), CE-DRW (Cross entropy Dynamic reweighting) (Cao et al., 2019), LDAM-DRW (label-distribution-aware margin loss) (Cao et al., 2019), BS (balanced soft-max) (Ren et al., 2020) and RIDE (Wang et al., 2021) for the CIFAR-100-LT dataset following the general settings outlined in Cao et al. (2019). Specifically, we use ResNet-32 (He & Garcia, 2009) as the backbone network. The network is trained using stochastic gradient descent (SGD) with a momentum of 0.9 and a weight decay of 0.0002. The initial learning rate is set to 0.1 and a linear learning rate warm-up is applied during the first 5 epochs to reach the initial learning rate. The training process spans over 200 epochs, during which the learning rate is decayed at the 160th and 180th epochs by a factor of 0.01. The hyper parameters: acceptance rate, augmentation probability and Number of test samples were 0.6, 0.5 and 10 respectively. The anticipated outcome was a consistent rise in validation accuracy across all five models and three imbalance ratios upon employing CUDA. In our reproduction of this study we were

ALGORITHM	IR=100	IR=50	IR=10	IR=100			IR 50			IR 10	
				Many	Med	few	Many	Med	few	Many	few
CE	38.49	42.92	56.61	65.8	36.27	8.43	63.8	34.73	13.83	63	42.53
CE+CMO	42.08	46.93	60.08	68.87	41.23	11.7	67.47	38.73	18.53	66.4	45.83
CE + CUDA	42.27	46.91	59.79	70.47	41.93	9.6	69.17	38.59	14.83	66.7	44.27
CE + CMO + CUDA	43.01	48.14	58.62	70.2	42.47	11.77	68.6	40.03	19.6	65.5	43.17
CE-DRW (Cao et al., 2019)	40.86	46.22	57.83	62.33	41.2	15.23	61.63	40.17	24.57	62.1	48.13
CE-DRW + Remix (Chou et al., 2020) [†]	45.8	49.5	59.2	~	~	~	~	~	~	~	~
CE-DRW + CUDA	47.23	51.9	61.76	62.5	49.2	27.03	62.3	48.3	36.17	64.2	56.1
LDAM-DRW (Cao et al., 2019)	42.48	47.15	57.96	62.17	42.43	19.4	62.43	41.07	25.8	63.3	45.9
LDAM + M2m (Kim et al., 2020) [‡]	43.5	~	57.6	~	~	~	~	~	~	~	~
LDAM-DRW + CUDA	47.52	50.57	58.18	66.43	50.27	22.03	66.07	45.63	26.3	63.33	46.6
BS (Ren et al., 2020)	42.24	45.99	58.29	59.63	41.33	22.8	58	41	29.87	61.5	51
BS + CUDA	47.47	52	61.52	63.03	48.8	27.83	62.53	47.03	39	64.13	55.53
RIDE (3 experts) (Wang et al., 2021) [†]	48.6	51.4	59.8	~	~	~	~	~	~	~	~
RIDE (3 experts)	48.87	51.95	59.13	67.7	50.17	25.27	67.2	46.5	29.3	64.9	46.1
RIDE + CMO (Park et al., 2022) [†]	0	53	60.2	~	~	~	~	~	~	~	~
RIDE + CMO	49.61	52.78	59.91	68.03	50.9	26.47	67.23	47.17	32.37	65.3	47.73
RIDE (3 experts) + CUDA	49.53	53.58	61.21	68.23	50.7	24.63	67.7	49	31.6	66.24	50

Figure 3: Validation accuracy on CIFAR-100-LT dataset. [†] are from Park et al. (2022) and [‡],* are from the original papers (Kim et al. (2020); Zhu et al. (2022)). Other results are from our implementation. We report the average results of three random trials on each combination of model and imbalance ratio. The first three column represents the overall accuracy for each imbalance ratio. The subsequent three groups of three columns represent the accuracy of the three groups of classes split as Many (the majority classes), few (the minority classes) and Med (the intermediate classes). The rows highlighted in green refer to the versions where CUDA is used. We can observe an increase in accuracy when we compare similar models with and without CUDA. For example vanilla CE+CMO for imbalance ratio 100 has accuracy 42.08 whereas CE+CMO+CUDA has accuracy of 43.01.

able to reproduce the accuracy values with a maximum deviation of 2.4%. Further we can observe from figure 3 a consistent increase in accuracy across all 5 models for the imbalance ratios 100 and 50 when paired with CUDA compared to the Vanilla edition. However for the imbalance ratio 10 we see a minor improvement in accuracy for all models except when CUDA is paired with CE+CMO.

4.1.2 Dynamics of LoL Score

We plot the progression of LoL scores (the strength of augmentation) for various classes across five models: CE, CE-DRW, BS, LDAM-DRW, and RIDE. The anticipated outcome was a stark difference between the LoL scores of majority class (0-49) and minority class (50-99) with LoL score of majority class being greater. In our reproduction of this study while there isn't a linear drop in augmentation strength as we move along the y-axis, there's a clear trend of higher average augmentation strength for the majority classes (0-49) compared to minority classes (50-99). The heat maps presented in Figure 4 validate the assertion that "Stronger augmentation on majority classes and weaker augmentation on minority classes yields better performance". In addition to this we observe a notable surge in LoL scores across most classes occurs after the 160th epoch, likely attributable to the decay in learning rate beyond this epoch.

4.1.3 Variance of Weight L1-norm

Image recognition can be considered to be a coupling of two tasks: feature learning where we extract features from the images and embed it into a feature space and classifier learning where we train a classifier over the learned features (Kang et al., 2020). The long-tailed data distribution can corrupt the representation space, where the distance between head and tail categories is much larger than the distance between two tail categories (Fu et al., 2023). A naively trained model on long-tailed class distributed data tends to have "artificially" large weights for the head classes. This yields a wider classification boundary in feature space for the head classes, allowing the classifier to have much higher accuracy on head classes, but hurting the performance of the tail classes (Kang et al., 2020).

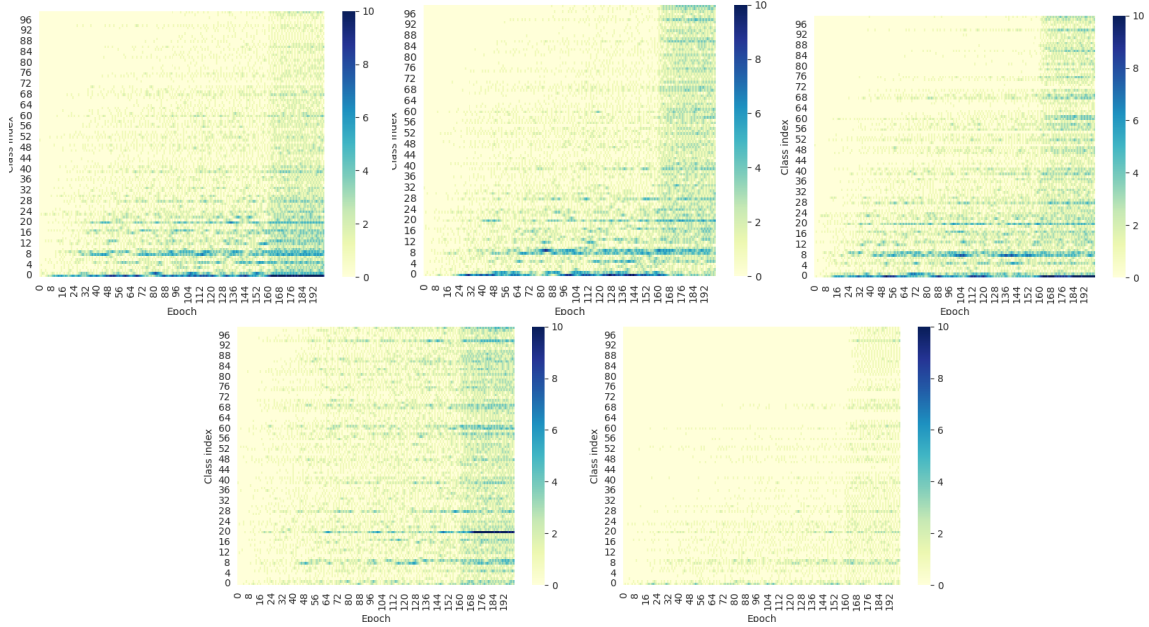


Figure 4: Evolution of LOL score in the order CE,CE-DRW,LDAM-DRW,BS,RIDE over the epochs.The x-axis represents the epochs, with the 200th epoch positioned on the rightmost side of each graph. The y-axis will display the classes, arranged in descending order based on the number of samples in each class.The intensity of the color of the heatmap represents the strength of augmentation.It is evident that during training the majority classes(0-49) have a stronger augmentation compared to the minority classes(50-99).

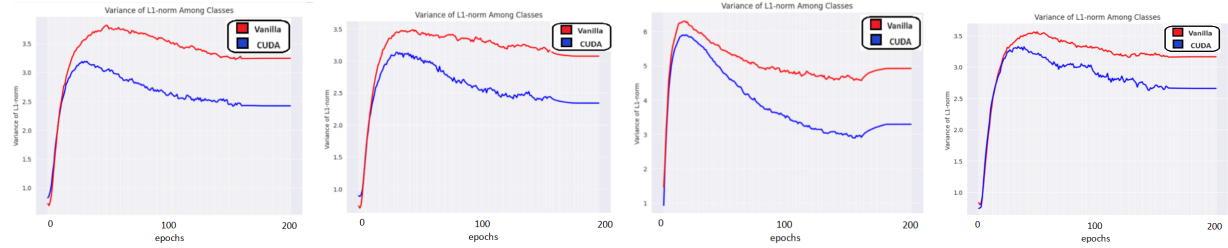


Figure 5: Variation Of weight-L1 norm in the order CE,CE-DRW,LDAM-DRW,BS over the epochs.The value of variance at epoch 200 represents the final value of variance of weight-L1 norm after training.It is evident that CUDA (indicated by the blue line) exhibits lower variance of weight-L1 Norm compared to the vanilla version (depicted by the red line).

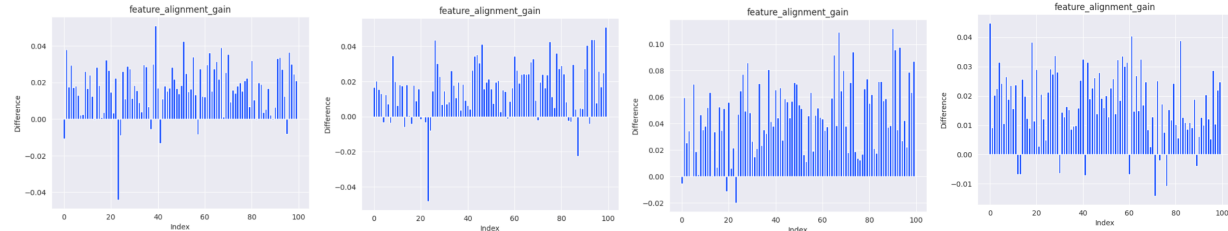


Figure 6: Feature alignment gain in the order CE,CE-DRW,LDAM-DRW,BS. Feature alignment gain is the increase in the average feature cosine similarity between feature vectors belonging to the same class.The x axis represents the classes and y axis represents the feature alignment gain for that class.It is evident that CUDA exhibits a positive feature alignment gain(indicated by the blue line) for most of the classes across all 4 models.

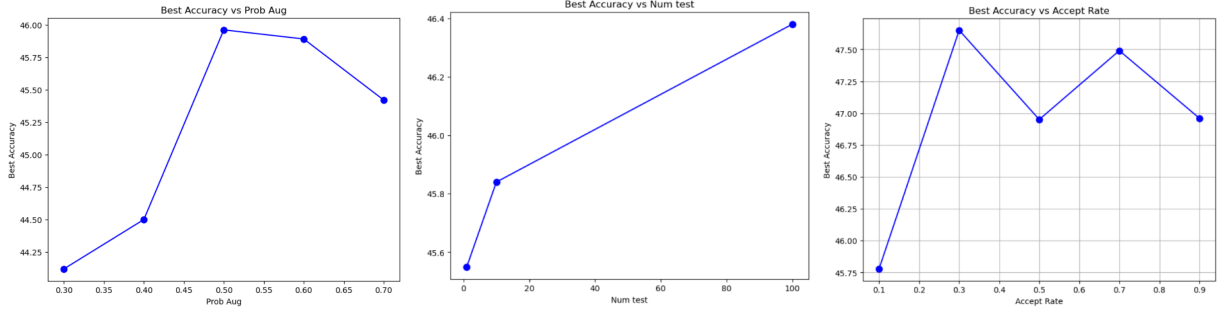


Figure 7: Hyper parameter Analysis of CUDA when paired with the model LDAM-DRW. The left most graph represents the sensitivity of accuracy with Augmentation probability. We see a concavity in performance when value of Prob Aug is changed between 0.3 to 0.7. The middle graph represents the sensitivity of accuracy with Number of test samples. We see a slight change in accuracy when value of Num Test is changed. The rightmost graph represents the sensitivity of accuracy with Acceptance rate. We see a concavity in performance when value of Accept rate is changed between 0.1 to 0.9.

The variance of classifier weight norm is usually used to measure how balanced the classifier is considering the input from a class-wise perspective (Kang et al., 2021). A lower variance in weight L1 norm indicates that the classifier assigns similar importance to all classes. We analyze how CUDA affects standard deviation of weight L1 norm across the 4 models over the epochs. The anticipated result was a consistent reduction in the value of variance of weight L1 norm on using CUDA across all 4 models. In our reproduction of this study we observe that there is a significant decrease in the standard deviation of weight L1 norm when we use CUDA compared to the vanilla version from Figure 5 validating the results of the original study.

We can say any enhancements in performance can be attributed to either improved feature representation or a more effective classifier. In this case, since the classifier remains constant for each case, the improvements are likely due to CUDA optimizing the feature representation space. The variance in weight norm decreases implying a reduction in distinction between different classification boundaries (between two head classes or between two tail classes or between a head and a tail class). Specifically we can infer that CUDA is able to make the feature representation more balanced in terms of inter class distances (Song et al., 2015).

4.1.4 Feature Alignment Gain

Continuing from the discussion of an imbalanced feature space representation in subsection 4.1.3, another significant impact of class imbalance on the feature representation space is the vulnerability of a cluster containing instances of a tail class (Huang et al., 2016). Due to their sparse nature, these clusters which are expected to contain instances of the same class are more prone to invasion by imposter feature vectors from other classes present in neighbourhood.

Feature alignment gain serves as a metric to quantify the effectiveness of a feature extractor in embedding features into the feature space. Specifically, it measures the improvement in feature alignment, which is the sum of cosine similarities between pairs of feature vectors within a given class when CUDA is used. We analyze how CUDA affects feature alignment gain of each class across the 4 models over the epochs for the validation dataset. The anticipated result was a mostly positive feature alignment gain on using CUDA across all 4 models. In our reproduction of this study we observe from Figure 6 that feature alignment gain is positive for most of the classes when we use CUDA.

When feature vectors within a class exhibit high similarity, they tend to cluster closely together within the feature representation space. This closeness results in reduced intra class distance (Song et al., 2015), meaning that feature vectors belonging to the same class are positioned closer to each other. Consequently, the likelihood of intrusions from feature vectors of a foreign class is diminished.

4.1.5 Hyper-Parameter Analysis

The paper proposed training on RIDE but we went with LDAM-DRW as LDAM-DRW showed a higher increase in performance when paired with CUDA which means that the magnitude of change in performance with change in hyper parameter will be higher. For Acceptance-Rate we train the model LDAM-DRW with CUDA for 5 equally spaced values from 0.1 to 0.9. Accept rate of 0.1 means that threshold for accepting the augmented samples is low leading to higher augmentation strength. Accept rate of 0.9 means that threshold for accepting the augmented samples is high leading to lower augmentation strength. For Probability-augmentation we train the model LDAM-DRW with CUDA for 5 equally spaced values from 0.3 to 0.7. Probability-augmentation of 0.3 means that most of the original images is retained when forming the data-loader. Probability-augmentation of 0.7 means that most of the original images is replaced by the augmented images when forming the data-loader. The anticipated result was a concavity in the value of validation accuracy when values of Acceptance-Rate and Probability-augmentation are increased. In our reproduction of the hyper parameter analysis studies from Figure 7 we can observe that Acceptance-Rate and Probability-augmentation shows a concavity in the performance. For the hyper parameter number of test samples we train the model LDAM-DRW with CUDA for three different values of 1,10,100. The anticipated result was a steep increase in accuracy between 1 to 10 values of T and a slight increase between 10 to 100 values of T. In our reproduction of the hyper parameter analysis we can see that the performance increases slightly with increase in Number of Test samples from Figure 7.

4.1.6 Curriculum Learning

Curriculum Learning (CL) is a training strategy designed to enhance machine learning models by progressively exposing them to increasingly complex or challenging data during training. Previous works (Zhou et al., 2020) have shown that curriculum learning can improve accuracy of LTR models. In the context of the CUDA algorithm, the LOL (Learning Objective Level) scores for each class initially start at zero and are iteratively updated at the end of each epoch based on the model’s performance with augmented images. After 200 epochs, an optimal combination of LOL scores is achieved, leading to the final model performance. To assess the impact of curriculum learning on accuracy, a two-step approach is employed. In the first step, a model is trained using the standard CUDA procedure. Subsequently, the LOL scores obtained from this initial training run are extracted and utilized as fixed scores in a subsequent run. In this second run, the model is trained without updating the LOL scores. The anticipated result was a reduction in accuracy on the second run when CUDA is trained without curriculum learning. In our reproduction of this component analysis we can observe from Figure 8 that there is an decrease in performance across all 5 models when CUDA is trained without curriculum learning.

4.1.7 Classwise-Score

To examine the validity of class-wise augmentation of CUDA, we apply CUDA with the same strength of DA for all classes. Instead of computing LOL score class-wisely, we computed only one LOL score for the entire dataset by uniformly random sampling instances in the training dataset regardless of class. The anticipated result was a reduction in accuracy when CUDA is trained without classwise score. In our reproduction of this component analysis we can observe from Figure 8 a significant performance degradation of CUDA across all 5 models without class-wise score compared to CUDA.

4.1.8 Comparison with other Augmentation techniques

We compare the performance of CUDA with other augmentation techniques: Auto-Augmentation (CIFAR, ImageNet and SVHN policy) (Cubuk et al., 2019), Fast Auto-Augmentation (CIFAR, ImageNet and SVHN policy) (Lim et al., 2019), DADA (Li et al., 2020) and Rand-Augmentation (m=1, n=2) (Cubuk et al., 2020) for the model LDAM-drw. The anticipated result was that CUDA outperforms all other existing data augmentation techniques. In our reproduction of this comparison, figure 8 reveals that CUDA consistently outperforms all other augmentation techniques.

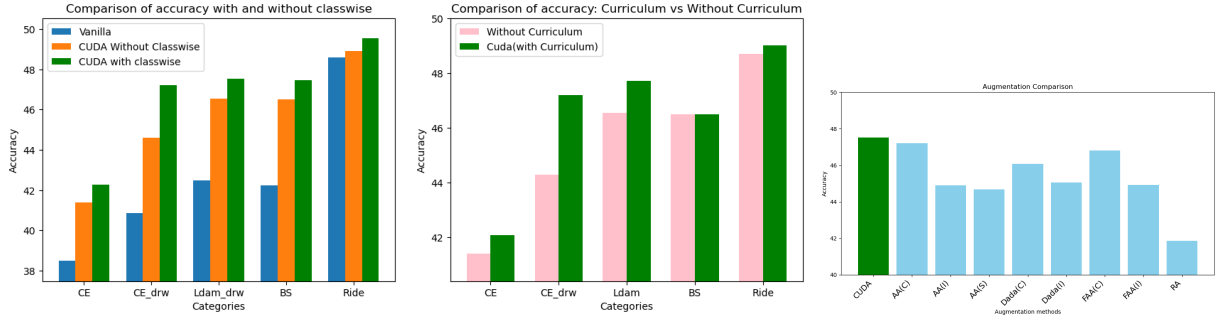


Figure 8: Component analysis on Classwise Score and Curriculum Learning, Comparison of accuracy on different augmentation techniques. The leftmost graph illustrates the comparison of accuracy among Vanilla, Cuda without Classwise Score and the original Cuda version with Classwise Score. The middle graph demonstrates the comparison of accuracy between Cuda without Curriculum Learning and the original Cuda version with Curriculum Learning. The rightmost graph represents the comparison of accuracy for 9 different augmentation methods Cuda, Auto Augmentation-CIFAR policy, Auto Augmentation-ImageNet policy, Auto Augmentation-SVHN policy, Dada-CIFAR, Dada-ImageNet, Fast Auto Augmentation-CIFAR, Fast Auto Augmentation-ImageNet policy and Random Augmentation. We observe that the original iteration of CUDA (represented by the green bar) consistently outperforms its competitors across all three studies.

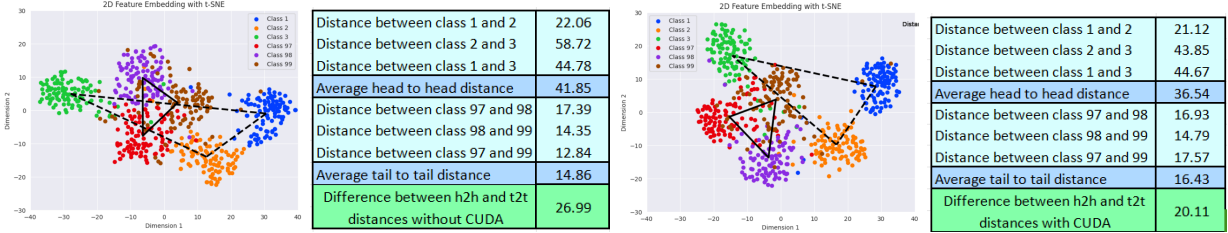


Figure 9: Leftmost-Feature representation of vanilla CE, inter class distances for vanilla CE, Feature representation of CE+CUDA, rightmost-inter class distances for CE+CUDA. In the feature representation space the red, purple and brown instances represent three tail classes (97, 98, 99) and the green, yellow and blue instances represent three head classes (1, 2, 3). The dotted line is connecting means of two heads and the solid line is connecting means of two tail classes. The distances in the table are measured between the means of the classes. It is evident that after using CUDA the difference between average head to head distance (h2h) and average tail to tail distance (t2t) has diminished.

4.2 Results beyond original paper

Section 4.2.1 delves into findings related to our third motivation of exploring the changes in feature representation space after using CUDA. The section 4.2.2 consists of an analysis on the performance of CUDA for the augmentation operation cutout which was implemented in the original code but not explicitly stated to be used in the paper. Section 4.2.3 consists of an analysis on accuracy gain when CUDA is used across three different imbalance ratios.

4.2.1 Quantitative and Qualitative analysis of feature embedding

We conducted an analysis of the feature embedding derived from the validation dataset of the imbalanced CIFAR-100-LT dataset, building upon prior methodologies (Huang et al., 2016), (Song et al., 2015) aimed at addressing class imbalance through enhanced feature representation. Specifically, we visualized the 2-dimensional feature representations of three head classes (1, 2, 3) and three tail classes (97, 98, 99) using t-SNE.

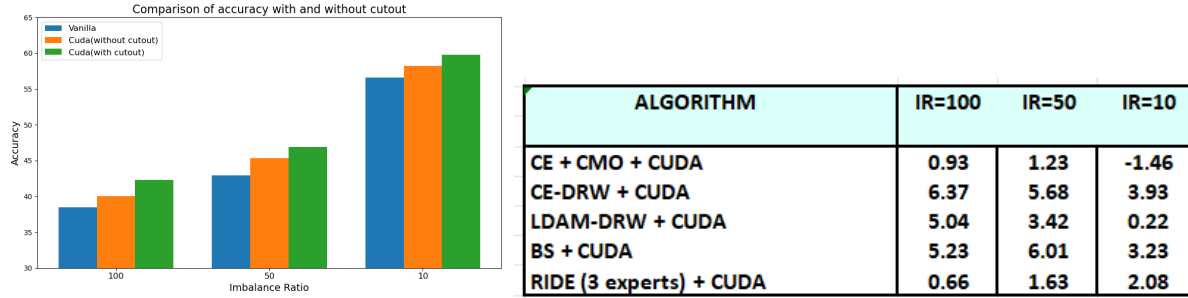


Figure 10: The left image represents the comparison of accuracy of CUDA when paired with cutout, when not paired with cutout and the vanilla version. The right image represents the analysis of gain in accuracy with 3 different versions of CIFAR-100-LT with imbalance ratio: 10, 50 and 100.

The quantitative aspect we examined was the variance in inter-class distances, as detailed in section 4.1.3. This variance can be quantified by the difference between the average distance within head classes and that within tail classes. Notably, we observed a diminished difference from the tables in Figure 9 when employing CUDA compared to the vanilla version, indicating an improvement in handling class imbalance.

The qualitative aspect we examined was the representation of the tail class clusters in the feature space. Following the adoption of CUDA, we noted that the clusters corresponding to tail classes exhibited greater coherence from Figure 9. There was a reduction in the intrusion of imposter vectors into these clusters, signifying enhanced separability. We also observe a slight increase in the average distance of means of tail classes denoting a wider classification boundary than before between tail classes.

4.2.2 Cutout

The usage of the augmentation operation Cutout was not explicitly mentioned in the original paper. However, the official implementation of CUDA also had an argument to either use or not use the cutout operation. Cutout has proved to improve generalization performance of CNNs (DeVries & Taylor, 2017). Our analysis focused on investigating how Cutout affects the performance of CUDA for the CE (cross-entropy) model to validate the fact that original authors used cutout during training for all models. Our findings in Figure 10 suggest that incorporating cutout during training is crucial for achieving the reported accuracy levels stated in the original paper for all models.

4.2.3 Gain in accuracy for imbalance ratio

We conducted a comparative analysis of the gain in accuracy among five models when paired with CUDA across three different imbalance ratios: 100, 50, and 10. Imbalance ratios reflect the disparity in class distribution within the dataset, with higher ratios indicating more pronounced class imbalances. Our findings in Figure 10 reveal a general trend where the gain in accuracy diminishes as the imbalance ratio decreases. We can infer that CUDA performs better when the imbalance ratio of the dataset is higher.

5 Discussion

The experimental results presented in the paper effectively supports the first claim of the original paper, demonstrating that applying an algorithm to find classwise augmentation strength can show improvements in validation accuracy (section 4.1.1). However, the performance of CUDA with model BCL couldn't be fully evaluated due to inadequate time. Nevertheless, we can still validate the first claim based on the available data. The heatmaps depicted in Figure 4 illustrate the progression of augmentation strength over the epochs, serving to validate the second assertion of the original paper. Initially, there exists a contrast in the LOL scores between the majority classes (0-49) and minority classes (50-100) before the 160th epoch. However, after training for 200 epochs, this contrast diminishes significantly. A holistic view of the evolution of LOL scores across epochs (section 4.1.2) still corroborates the second claim of the original paper, that

employing stronger augmentation on majority classes and milder augmentation on minority classes yields superior model performance compared to the opposite strategy.

By analyzing the variance of weight L1-norm(section 4.1.3),the reproduction study showcases how CUDA effectively addresses the imbalance problem reducing the variance leading the model to assign equal importance to each class as claimed in the original paper.Through our analysis, we inferred that CUDA enhances the balance of feature representation in terms of inter-class distances.Additionally, we reproduced the examination of feature alignment gain (section 4.1.4), further affirming CUDA’s efficacy in addressing the imbalance problem by increasing the feature alignment as claimed in the original paper.Through our analysis,we inferred that CUDA reduces the intra-class distances between instances of the same class specifically the tail classes.To validate these two deductions regarding balanced inter-class distances and reduced intra-class distances, we compared the feature representation space of the vanilla and CUDA versions (section 4.2.1).Our analysis confirmed both inferences, indicating that CUDA enhances feature representation by promoting balance in inter-class distances and diminishing the intrusion of foreign instances by reducing intra-class distances.

The Hyper-parameter sensitivity analysis for augmentation probability and Accept rate on validation accuracy reveals a concavity as claimed by the original paper(Figure 7).The impact of curriculum and classwise score on the performance of CUDA is evident from our findings in (section 4.1.6 and section 4.1.7) validating their importance in performance of CUDA as claimed by the original paper.We found that cutout augmentation plays a significant role in the accuracy gain observed when using CUDA, even more so than curriculum learning or classwise score(section 4.2.3).We claim the original authors had used cutout during training across all models but have not explicitly stated in the paper.The stated values of accuracy in the original paper can only be attained when CUDA is used with cutout augmentation.Our analysis on the imbalance ratio indicates that CUDA’s efficiency diminishes as we move towards datasets with lower imbalance(section 4.2.3).From this, we can also infer that CUDA does not provide significant improvements with balanced datasets.

5.1 What was easy and what was difficult

The paper was really easy to follow. The section on the repository for CIFAR-100-LT was clearly written.The description of the arguments that we pass during training was properly stated.The algorithm which makes up CUDA was completely logical in its implementation.The lack of significant barriers in setting up the code enhances its portability.The dependencies were not clearly mentioned by the author requiring additional time to find the versions by trial and error.The original paper had also included performance comparison on datasets ImageNet-LT and Inaturalist-18,the section of the original repository for ImageNet-LT and Inat-18 contains redundant code and uncleaned up code.The paper claims to deviate from the model recipes of BCL and NCL to ensure a fair comparison.However, it fails to clearly state these deviations, making it difficult to assess their performance in this study.

5.2 Communication with original authors

The initial attempts to contact the authors through the email IDs given in the paper was not successful.We were able to contact the authors through linked-in in latter half of the study.The authors were able to clarify our doubts on implementing the component analysis for curriculum learning and class-wise score.Regrettably,the authors were unable to provide a clear recipe for BCL.

References

- Sumyeong Ahn, Jongwoo Ko, and Se-Young Yun. Cuda: Curriculum of data augmentation for long-tailed recognition, 2023.
- Mateusz Buda, Atsuto Maki, and Maciej A Mazurowski. A systematic study of the class imbalance problem in convolutional neural networks. *Neural networks*, 106:249–259, 2018.

- Kaidi Cao, Colin Wei, Adrien Gaidon, Nikos Arechiga, and Tengyu Ma. Learning imbalanced datasets with label-distribution-aware margin loss. *Advances in neural information processing systems*, 32, 2019.
- Ekin D Cubuk, Barret Zoph, Dandelion Mane, Vijay Vasudevan, and Quoc V Le. Autoaugment: Learning augmentation strategies from data. In *Proceedings of the IEEE/CVF Conference on Computer Vision and Pattern Recognition*, pp. 113–123, 2019.
- Ekin D Cubuk, Barret Zoph, Jonathon Shlens, and Quoc V Le. Randaugment: Practical automated data augmentation with a reduced search space. In *Proceedings of the IEEE/CVF conference on computer vision and pattern recognition workshops*, pp. 702–703, 2020.
- Terrance DeVries and Graham W Taylor. Improved regularization of convolutional neural networks with cutout. *arXiv preprint arXiv:1708.04552*, 2017.
- Siming Fu, Xiaoxuan He, Xinpeng Ding, Yuchen Cao, and Hualiang Wang. Uniformly distributed category prototype-guided vision-language framework for long-tail recognition, 2023.
- Haibo He and Edwardo A Garcia. Learning from imbalanced data. *IEEE Transactions on knowledge and data engineering*, 21(9):1263–1284, 2009.
- Chen Huang, Yining Li, Chen Change Loy, and Xiaoou Tang. Learning deep representation for imbalanced classification. In *2016 IEEE Conference on Computer Vision and Pattern Recognition (CVPR)*, pp. 5375–5384, 2016. doi: 10.1109/CVPR.2016.580.
- Bingyi Kang, Saining Xie, Marcus Rohrbach, Zhicheng Yan, Albert Gordo, Jiashi Feng, and Yannis Kalantidis. Decoupling representation and classifier for long-tailed recognition. In *International Conference on Learning Representations*, 2020. URL <https://openreview.net/forum?id=r1gRTCvFvB>.
- Bingyi Kang, Yu Li, Sa Xie, Zehuan Yuan, and Jiashi Feng. Exploring balanced feature spaces for representation learning. In *International Conference on Learning Representations*, 2021. URL <https://openreview.net/forum?id=0qtLIabPTit>.
- Jaehyung Kim, Jongheon Jeong, and Jinwoo Shin. M2m: Imbalanced classification via major-to-minor translation. In *Proceedings of the IEEE/CVF conference on computer vision and pattern recognition*, pp. 13896–13905, 2020.
- Yonggang Li, Guosheng Hu, Yongtao Wang, Timothy Hospedales, Neil M Robertson, and Yongxin Yang. Differentiable automatic data augmentation. In *European Conference on Computer Vision*, pp. 580–595. Springer, 2020.
- Sungbin Lim, Ildoo Kim, Taesup Kim, Chiheon Kim, and Sungwoong Kim. Fast autoaugment. *Advances in Neural Information Processing Systems*, 32, 2019.
- Seulki Park, Youngkyu Hong, Byeongho Heo, Sangdoo Yun, and Jin Young Choi. The majority can help the minority: Context-rich minority oversampling for long-tailed classification. In *Proceedings of the IEEE/CVF Conference on Computer Vision and Pattern Recognition*, pp. 6887–6896, 2022.
- Jiawei Ren, Cunjun Yu, Xiao Ma, Haiyu Zhao, Shuai Yi, et al. Balanced meta-softmax for long-tailed visual recognition. *Advances in neural information processing systems*, 33:4175–4186, 2020.
- Hyun Oh Song, Yu Xiang, Stefanie Jegelka, and Silvio Savarese. Deep metric learning via lifted structured feature embedding, 2015.
- Xudong Wang, Long Lian, Zhongqi Miao, Ziwei Liu, and Stella Yu. Long-tailed recognition by routing diverse distribution-aware experts. In *International Conference on Learning Representations*, 2021. URL <https://openreview.net/forum?id=D9I3drBz4UC>.
- Boyan Zhou, Quan Cui, Xiu-Shen Wei, and Zhao-Min Chen. Bbn: Bilateral-branch network with cumulative learning for long-tailed visual recognition. In *Proceedings of the IEEE/CVF conference on computer vision and pattern recognition*, pp. 9719–9728, 2020.

Table 1: Operation Parameter Description

Operation	Description
Flip On/Off	Flip top and bottom
Mirror On/Off	Flip left and right
Edge Enhancement On/Off	Increasing the contrast of the pixels around the targeted edges
Detail On/Off	Utilize convolutional kernel $\begin{bmatrix} 0 & -1 & 0 \\ -1 & 10 & -1 \\ 0 & -1 & 0 \end{bmatrix}$
Smooth On/Off	Utilize convolutional kernel $\begin{bmatrix} 1 & 1 & 1 \\ 1 & 5 & 1 \\ 1 & 1 & 1 \end{bmatrix}$
AutoContrast On/Off	Remove a specific percent of the lightest and darkest pixels
Equalize On/Off	Apply non-linear mapping to make uniform distribution
Invert On/Off	Negate the image
Gaussian Blur	Blurring an image using Gaussian function with radius [0,2]
Resize Crop	Resizing and center random cropping with scale [1,1.3]
Rotate	Rotate the image with angle [0,30]
Posterize	Reduce the number of bits for each channel in the range [0,4]
Solarize	Invert all pixel values above a threshold in the range [0,256]
SolarizeAdd	Adding value and run solarize in the range [0,110]
Color	Colorize gray scale values in the range [0.1, 1.9]
Contrast	Adjust the distance between colors in the range [0.1,1.9]
Brightness	Adjust image brightness in the range [0.1,1.9]
Sharpness	Adjust image sharpness in the range [0.1,1.9]
Shear X	Shearing X-axis in the range [0,0.3]
Shear Y	Shearing Y-axis in the range [0,0.3]
Translate X	Shift X-axis in the range [0,100]
Translate Y	Shift Y-axis in the range [0,100]

Jianggang Zhu, Zheng Wang, Jingjing Chen, Yi-Ping Phoebe Chen, and Yu-Gang Jiang. Balanced contrastive learning for long-tailed visual recognition. In *Proceedings of the IEEE/CVF Conference on Computer Vision and Pattern Recognition*, pp. 6908–6917, 2022.

A Augmentation preset

We use 22 different augmentation operations for CUDA each having their own parameter. The details of each of these operation has been described in table 1. The magnitude parameter divides the augmentation parameter into 30 values linearly. For example for Rotate max value is 30 and min value is 0, the magnitude of parameter for rotate is defined by

$$m_{\text{rotate}}(s) = (30 - 0)/30 * s, \text{ thus } m_{\text{rotate}}(1) = 1 = (30 - 0)/30 * 1$$

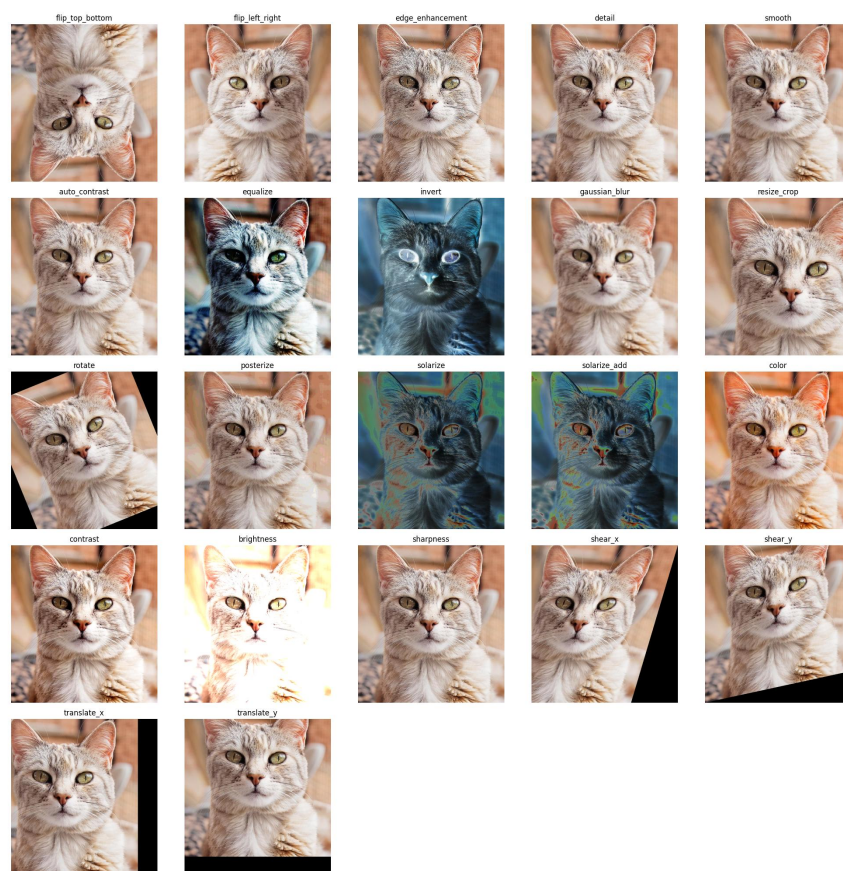


Figure 11: The 22 augmentation operations we use for CUDA